

Cracking and deformation of RC beams strengthened with Reactive Powder Composites

I. Ujike, H. Sogo & D. Takasuga

Ehime University, Graduate school of science and engineering, Matsuyama, Ehime, Japan

Y. Konishi & M. Numata

Aikyo Corporation, Toon, Ehime, Japan

ABSTRACT: A reinforced concrete beam without cracking under serviceability limit state has been developed. A part of the tension zone in the reinforced concrete beam was fortified with Reactive Powder Composite (RPC). Flexural load tests on the beam were carried out in this study. The cracking moment of the beam reinforced with RPC could be estimated by the elastic theory, provided that the stress due to the restraint of reinforcing bar against the autogenous shrinkage of RPC must be taken into consideration. After the generation of cracking, RPC has little effect on the deformation of beam reinforced with RPC due to the increase of bending moment. However, the flexural capacity of beam fortified with RPC is larger than that of the reinforced concrete beam without RPC and increases with the increase in the reinforced area of RPC.

1 INTRODUCTION

Cracks developed in a reinforced concrete member speed up the deterioration of the reinforced concrete member, because cracks make the invasion of harmful substances easy. It is difficult to evaluate the geometrical properties of the crack quantitatively by the irregularity of the crack. Therefore, an estimate method for durability of reinforced concrete members in consideration of the effect of the crack hasn't been established. Although crack width is controlled to stay within the permissible crack width by the usual design, the crack is a weak point even if it is narrow. In order to give the reinforced concrete member high durability, it is necessary to avoid cracking.

Recently, Ductile Fiber Reinforced Cementitious Composites (DFRCC) which destruction energy and ductility improve greatly under tensile stress condition have been developed (JCI 2002). Reactive Powder Composite (RPC) is one of DFRCC and the paste of RPC is made super high strength by the use of reactive powder, fine granulating of aggregate and tightest filling of powder (Musha et al 2002). From this, the stress which a crack occurs in first after elastic deformation by the action of tensile force, first cracking strength, is very high about 8 N/mm².

Authors gave attention to super high first cracking strength of RPC. A reinforced concrete beam without cracking under serviceability limit state has been developed (Ujike et al. 2005). The part of tension zone in the reinforced concrete beam

was strengthened with RPC. In this study, flexural loading tests on the beams were carried out and cracking moment, curvature, reinforcement strain and flexural capacity of the beams fortified by RPC were investigated.

2 EXPERIMENTS

2.1 Materials

RPC used in this study consists of premixed powder in a carefully selected combination of cement, silica particles and siliceous sand and steel fibers, without coarse aggregate. Special water reducing agent was added to mixing water. For conventional concrete, high early strength portland cement (density 3.14 g/cm³) was used. Crushed sand (density of surface-dry 2.57g/cm³, absorption 1.33%) and crushed gravel (density of surface-dry 2.62 g/cm³, absorption 0.88%) were used as a fine and coarse aggregate, respectively. Water reducing agent was also used.

2.2 Specimen

Beam specimens were produced for a flexural loading test. Specimens have the height of 200mm, the width of 150mm and overall length of 1800mm. Details of cross sections are illustrated in Fig.1. In figure, a gray part shows RPC. Deformed bars with a bar diameter of 16mm were used as a primary tension reinforcement. For DRC80, DRC50 and DRC30, reinforcing bars were arranged in the center of height direction of the RPC part. Deformed bars

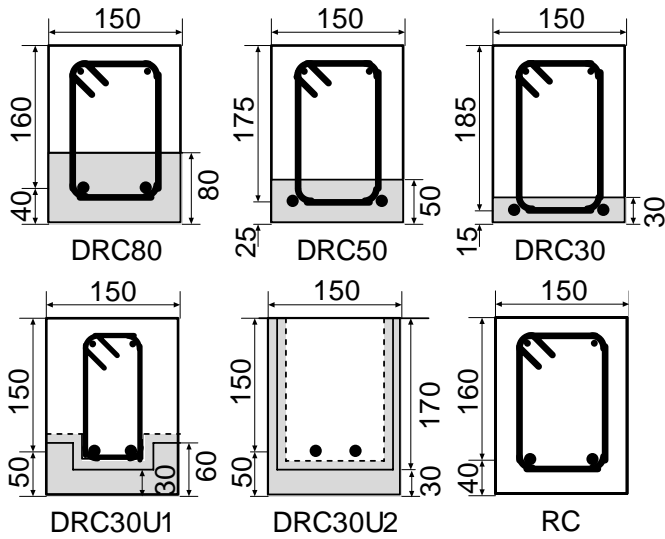


Figure 1. Cross – sections of specimens

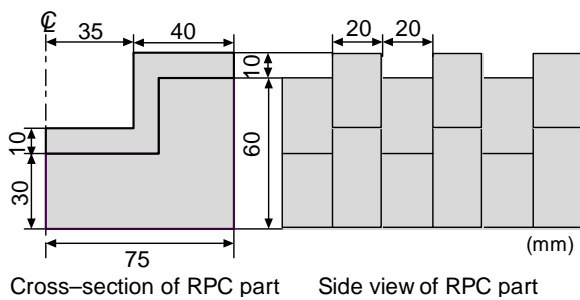


Figure 2. Outline of irregularity on RPC (DRC30U1)

with a bar diameter of 10mm were used as a stirrup and were arranged along the entire length of the specimen at 100mm spacing. These stirrups also have the function to prevent the slip between concrete and RPC in addition to the function of shear reinforcement. For DRC30U1 and DRC30U2, the bottom and the side sections except for reinforcing bars in the beam were fortified in the concavity-shaped. This arrangement of steel bars, as described later, has the function to decrease the influence of the autogenous shrinkage of RPC on the cracking moment of the beams. Furthermore, convex parts with height of 1cm and width of 2cm were formed on the RPC surface in contact with concrete at intervals of 2cm, as shown in Fig.2.

The specified mix proportions of RPC and concrete are tabulated in Table 1 and Table 2, respectively. The beams reinforced with RPC were produced with the following process. Assembled steel bars were fixed within a form. For DRC30U1 and DRC30U2, the concrete part in the beam was made from polystyrene foam. The polystyrene foam was turned upside down and was placed in the form. RPC having the flow value of 270mm was mixed and RPC was cast into the form with vibration. After 48 hours from casting of RPC, the polystyrene foam was removed from RPC and RPC specimens were steam-cured at 98 degrees C for 48 hours. Concrete was constructed on RPC part after 3 days from the finish of steam curing and a reinforced concrete

Table 1. Specified mix proportion of RPC

Water powder ratio (%)	Unit content (kg/m ³)			
	Water	Premix powder	Steel fiber	SP*
8.0	180	2254	157	27

*Special water reducing agent

Table 2. Specified mix proportion of concrete

W/C (%)	s/a (%)	Unit content (kg/m ³)			
		Water	Cement	Fine aggregate	Coarse aggregate
45.0	35.0	165	367	645	1219

Table 3. Mechanical properties of RPC and concrete

Specimen	RPC (N/mm ²)			Concrete (N/mm ²)	
	f_D	f_{cr}	E_D	f_c	E_c
DRC80	193.0	14.1	53830	32.4	28130
DRC50	193.0	14.1	53830	45.9	31680
DRC30	193.0	14.1	53830	45.9	31680
DRC30U1	179.3	11.8	52270	35.4	25420
DRC30U2	213.5	11.1	55510	44.8	29050
RC	-----	-----	-----	45.9	31680

f_D : Compressive strength of RPC

f_{cr} : First crack strength of RPC

E_D : Elastic modulus of RPC

f_c : Compressive strength of concrete

E_c : Elastic modulus of concrete

beam without RPC was also constructed at the same time, and subsequently left motionless in the laboratory until a loading test. Table 3 shows the mechanical properties of RPC and concrete used for each specimen. The mechanical properties were measured at the time of the loading test.

2.3 Loading test

Flexural loading tests were performed after 7 – 10 days from the cast of concrete. Fig.3 shows the side view of a specimen and the loading points. As shown in Fig.3, the load was applied at two positions which divide the span into three equal and gradually increased in 2kN steps. Reinforcement strain, concrete strain at upper fiber, RPC strain at bottom fiber, strains at the adjacent joint between RPC and concrete, deflection and crack width were measured in the tested zone with the length of 500mm subjected to pure bending. Fig.4 shows the

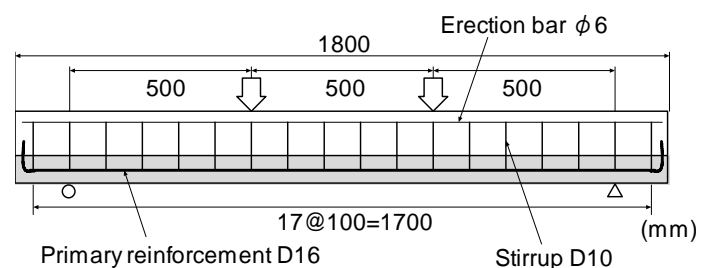


Figure 3. Side view of specimen and loading point

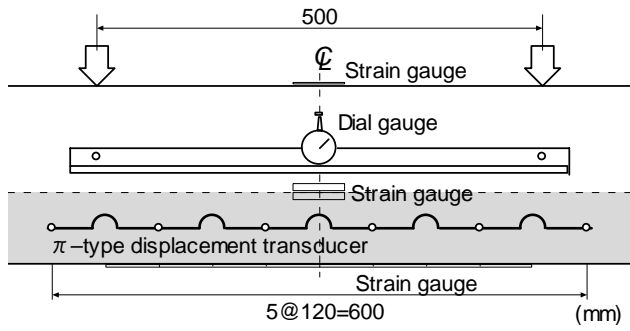


Figure 4. Outline of measurement

outline of measurement. The reinforcement strain was measured by strain gauges fixed at the center of a steel bar. The deflection was measured with dial gauges having the accuracy of 1/1000mm. For measurement of the RPC strain, nine strain gauges with the length of 60mm were affixed at the bottom surface of the specimen. In the cases of DRC80, DRC50 and DRC30, strains adjacent the joint between RPC and concrete were measured. Crack widths were measured with a π -type displacement transducer having the accuracy of 1/2000mm.

3 EXPERIMENTAL RESULTS AND DISCUSSION

3.1 Cracking moment

In this study, the serviceability limit state for cracks is investigated. In order to evaluate the performance on crack prevention of the beam reinforced with RPC, the moment corresponding to the permissible crack width is calculated as the external moment to act under the serviceability limit state. The moment corresponding to the permissible crack width is calculated based on Standard Specification for Design and Construction of Concrete Structure (JSCE 2002) (hereafter referred as Specification).

According to Specification, when environmental condition regarding the corrosion of reinforcement is normal environment, the permissible crack width w_a for the corrosion of reinforcement is given as a function of cover c :

$$w_a = 0.005c \quad (1)$$

As cover of RC shown in Fig.1 is 32mm, we obtain $w_a = 0.16$ mm. The following equation for crack width w has been proposed by Specification.

$$w = 1.1k_1k_2k_3\{4c+0.7(C_s-\phi)\}(\sigma_s/E_s+\varepsilon'_{cs}) \quad (2)$$

where, k_1 is a constant to take into account the difference in surface geometry of reinforcement, $k_1 = 1.0$ as deformed bar was used in this study. k_2 is a constant to take into account the influence of concrete strength f'_c , $k_2 = 0.93$ as k_2 is calculated by $k_2 = 15/(f'_c+20)+0.7$. k_3 is a constant for arrangement of reinforcement, $k_3 = 1.0$ as reinforcing bars are arranged in one layer. And C_s = center to center distance of reinforcing bar; ϕ = bar diameter; σ_s = reinforcement stress; E_s = modulus of elasticity of reinforcement. ε'_{cs} is the strain to take into account the influence of creep and drying shrinkage on crack width, $\varepsilon'_{cs} = 150 \times 10^{-6}$ is used in general. From Eq.(2), the reinforcement stress $\sigma_s = 159$ N/mm² is obtained. Furthermore, the relationship between moment M and reinforcement stress σ_s is given from elastic analysis with the assumption that tensile stress in concrete is negligible as follow:

$$\sigma_s = n(M/I_i)(d-x) \quad (3)$$

where, n = elastic modular ratio of steel bar to concrete; d = effective depth; x = neutral axis depth; I_i = moment of inertia of transformed cross section about neutral axis. Substituting $\sigma_s = 159$ N/mm² into Eq.(4), $M = 8.82$ kNm is obtained.

Fig.5 shows an example of the change of strains measured by the strain gauges affixed at a bottom

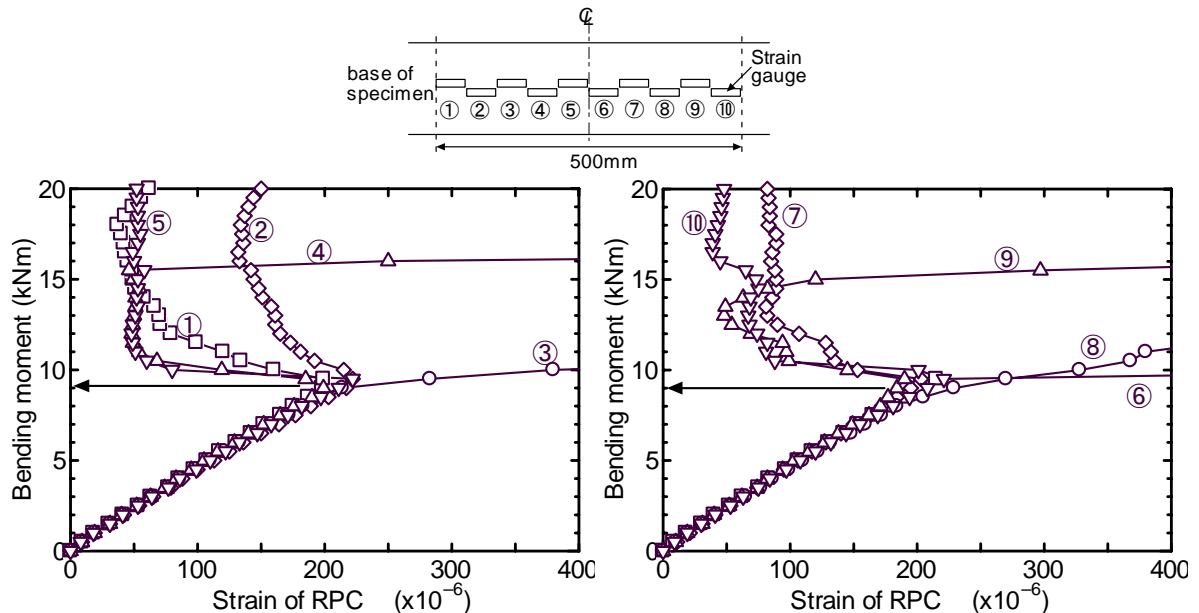


Figure 5. Strains of RPC at bottom fiber of DRC50

Table 4. Cracking moment of specimens reinforced with RPC

Specimen	Cracking moment (kNm)			$\sigma_{c,as}$ (N/mm^2)
	Measurement	Calculation I	Calculation II	
DRC80	10.15	13.13	10.31	3.04
DRC50	9.00	13.18	8.85	4.63
DRC30	6.00	12.68	6.29	7.12
DRC30U1	10.00	9.11	----	----
DRC30U2	8.89	8.99	----	----

$\sigma_{c,as}$:stress due to restraint of reinforcing bar against autogenous shrinkage of RPC

fiber of the beam with the increase of moment. The strains of RPC at the bottom fiber increase linearly until the generation of cracking. There are an increase and a decrease in strain of RPC rapidly due to the generation of cracking. In this study, the moment just before the strain changed remarkably is decided with the cracking moment. Table 4 shows the cracking moment of specimens reinforced with RPC. The cracking moments of the beams fortified with RPC except for DRC30 are larger than the moment corresponding to permissible crack width of RC, that is, it means that a crack doesn't occur in the beam appropriately reinforced with RPC under serviceability limit state.

The calculated values of the cracking moment for specimens reinforced with PRC are also shown in Table 4. The cracking moments of calculation I are obtained from the following equation based on elastic theory under the assumption that a crack generates when the tensile stress at the bottom fiber of the beam reaches the first crack strength of RPC.

$$M_{cr} = (f_{cr}I_g)/(h-y) \quad (4)$$

where, M_{cr} = cracking moment, f_{cr} = first crack strength of RPC, h = height of beam. y and I_g are depth of centroid and the moment of inertia of transformed cross section about centroid as already shown in Table 4. The calculations on DRC80,

DRC50 and DRC30 overestimate the cracking moment of specimen reinforced with RPC.

It has been reported that the autogenous shrinkage of RPC is large (Katagiri et al 2002). The effect of autogenous shrinkage of RPC is taken into consideration by the calculation on the cracking moment. $\sigma_{c,as}$ in Table 4 is the stress due to the restraint of a reinforcing bar against the autogenous shrinkage of RPC produced by the end of steam curing. It is assumed in the calculation of restraint stress that both RPC and a steel bar change in a body. From previous study (Katagiri et al 2002), the autogenous shrinkage strain used for the calculation is set 500×10^{-6} for RPC containing the steel fiber. The relaxation of the restraint stress by creep isn't taken into consideration, because creep of RPC is very small. In calculation II, the restraint stress was deducted from the first cracking strength, and except for this, it is the same way as the calculation I. The calculation II is comparatively well in agreement with the measurement. The cracking moment of the beam reinforced with RPC can be estimated by the elastic analysis in consideration of the restraint stress due to autogenous shrinkage of RPC.

From this fact, if the restraint stress can be made small, it expects that the resistance against cracks for the beam reinforced with RPC can be improved more. In DRC30U1 and DRC30U2, in order to reduce the restraint stress developed in RPC, the reinforcing bar isn't arranged in RPC. The cracking moments of DRC30U1 and DRC30U2 are equal or greater than that of DRC50, although the reinforcement area of RPC in the tension zone of the beam is small. And the calculated values of DRC30U1 and DRC30U2 are almost in agreement with the measured values.

3.2 Cracking

Fig.6 shows the crack width of RC and the displacement of RPC at the depth of the reinforcing bar of DRC80 and DRC30. About RC, one crack

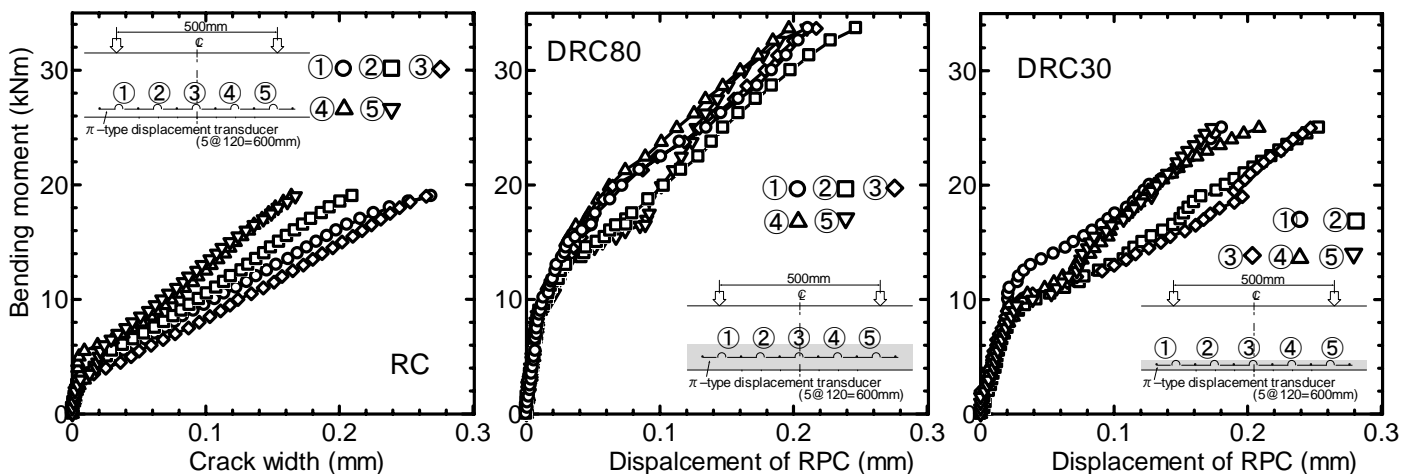


Figure 6. Crack width of RC and displacement of RPC at depth of reinforcing bar (DRC80, DRC30)

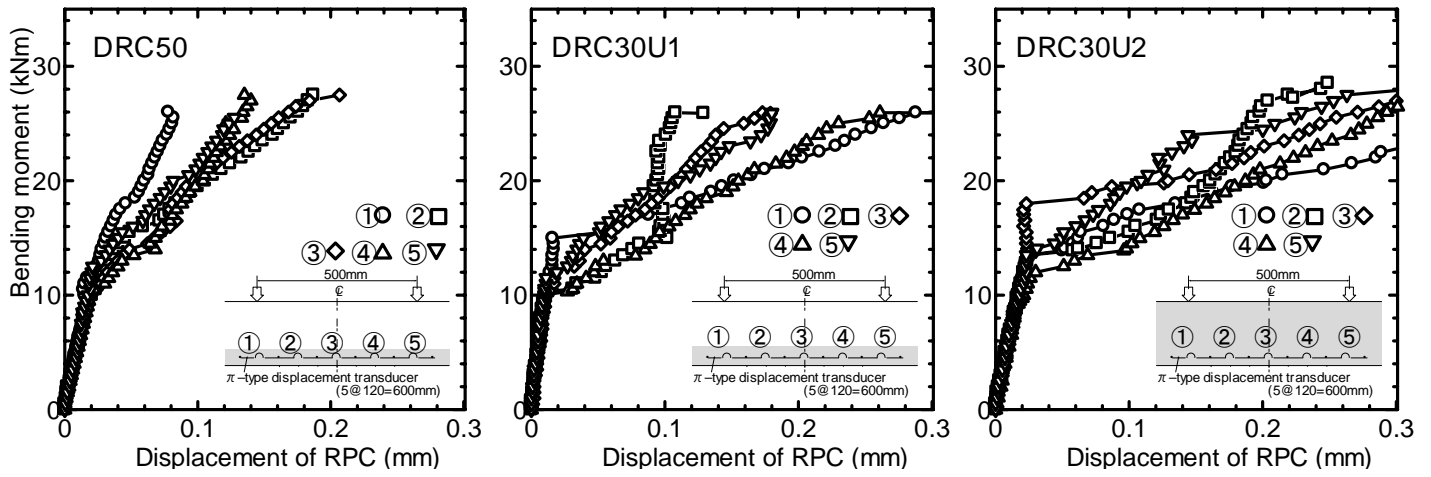


Figure 7. Displacement of RPC at depth of 25mm from bottom fiber (DRC50, DRC30U1, DRC30U2)

generated to the extent of measurement of one displacement transducer. The value shown in Fig.6 is the average of the value measured at the both sides of beam. About DRC80 and DRC30, The values shown in Fig.6 are also the average of the measured value of the displacement transducer of both sides of beam. However, several cracks were generated in the one measurement section. Therefore, at the failure of the beam, the width of one crack that was generated on the beam fortified with RPC is 0.1mm or less. The increase ratio of displacement of RPC to the increase in bending moment for DRC30 is larger than that for DRC80. The reason for this is that the effective depth of the reinforcing bar is large and the area of reinforcement with RPC is small.

Fig.7 shows the displacement of RPC at the depth of 25mm from the bottom fiber for DRC50, DRC30U1 and DRC30U2. About these beams, several cracks were also generated in the one measurement section. Although the cracking moment of DRC30U1 and DRC30U2 equals or is greater than that of DRC50, the increase ratio of displacement of RPC to the increase in bending moment for DRC30U1 and DRC30U2 is larger than

that for DRC50. This may be because the reinforcing bar isn't arranged inside RPC in DRC30U1 and DRC30U2.

3.3 Reinforcement strain

Fig.8 shows the strain of a reinforcing bar in the beams fortified with RPC. The broken line in Fig.8 is the calculation by elastic analysis in consideration of full section of the beam. The contribution of RPC is evaluated by the use of elastic modular ratio of RPC to concrete, like the case of steel bars in reinforced concrete. Before the generation of cracking, experimental values agree well with the calculated values. The dot-dash line is the calculation neglecting the tension zone of the beam. The measurement values are smaller than the calculation values due to the contribution of RPC after crack generating.

In order to consider the contribution of RPC, the softening stress – crack opening displacement (COD) relationship shown in Fig.9 is used in this study. The relationship was established by referring to the guidelines for design of DFRCC (JSCE 2004). From the measurement shown in Fig. 6 and Fig.7, it

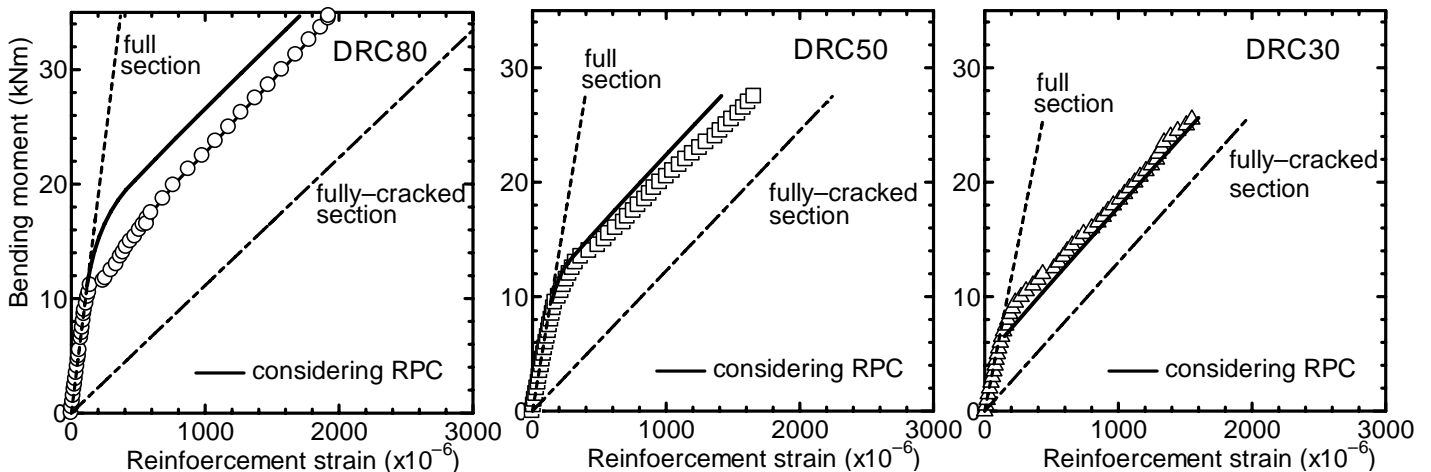


Figure 8. Reinforcement strain of beams fortified with RPC (DRC80, DRC50, DRC30)

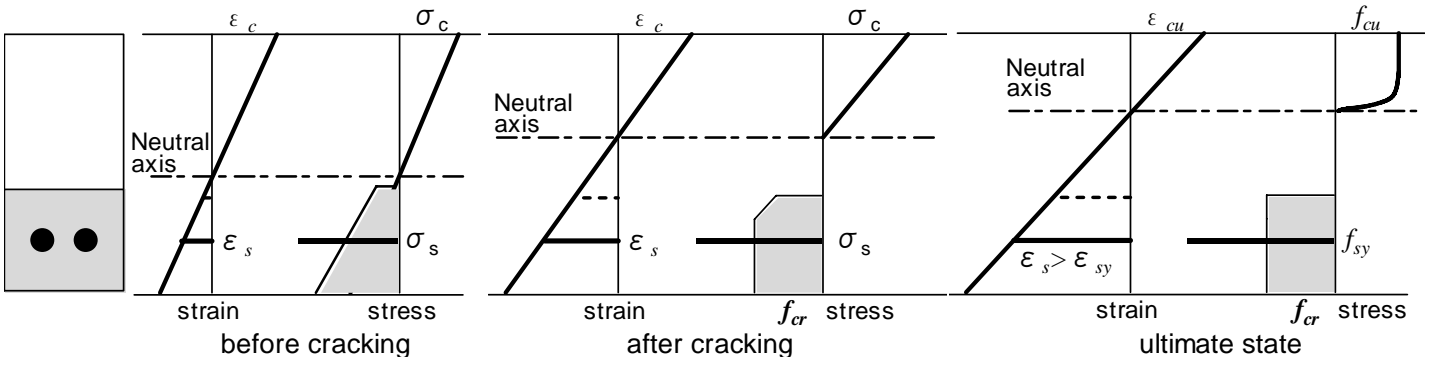


Figure 10. Distributions of strain and stress in beam fortified with RPC

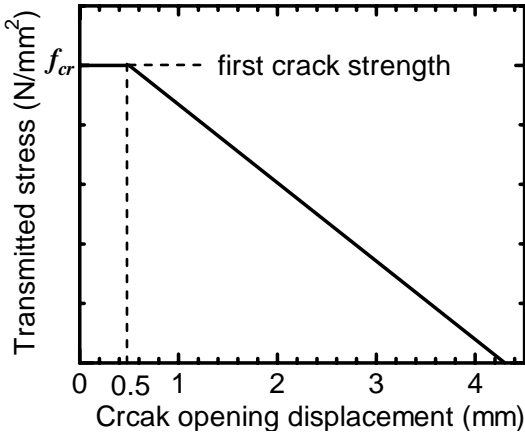


Figure 9. Tension softening diagram of RPC

is considered that the stress equivalent to first crack strength is developed in RPC after generating crack, because the crack width of RPC is as small as 0.1mm or less. Furthermore, based on this, the distributions of strain and stress at arbitrary section of the beam fortified with RPC are assumed as shown in Fig. 10. We have two equations for equilibrium of axial force and bending moment, therefore, concrete strain and reinforcing strain can be obtained by solving both equations simultaneously. The solid line in Fig.8 is the calculation value which takes the effect of RPC into consideration, as mentioned above. In calculation of

DRC80, when bending moment is not less than 20.3 kNm, the stress corresponding to first crack strength is distributed over the entire cross-section of the RPC part. About DRC50, it is 12.9 kNm or more and it is simultaneous with the generation of the crack about DRC30. The calculation value is comparatively well in agreement with the measurement value, although the calculated value tends to underestimate the measured value as the area of RPC in beam increases.

3.4 Curvature

Fig.11 and Fig.12 show comparisons of experimental and calculated changes of curvature with the increase of moment. About the calculation shown in the figures, I_g is the moment of inertia of transformed cross section about centroid. I_{cr} is the moment of inertia of fully cracked section transformed to concrete. It is assumed that tension of concrete and RPC is neglected when I_{cr} is calculated. I_e is the effective moment of inertia, and assuming cross section stiffness is constant all over the member length, I_e is computed by following equation (JSCE 2002).

$$I_e = \left(\frac{M_{cr}}{M_{max}} \right)^3 I_g + \left\{ 1 - \left(\frac{M_{cr}}{M_{max}} \right)^3 \right\} I_{cr} \quad (5)$$

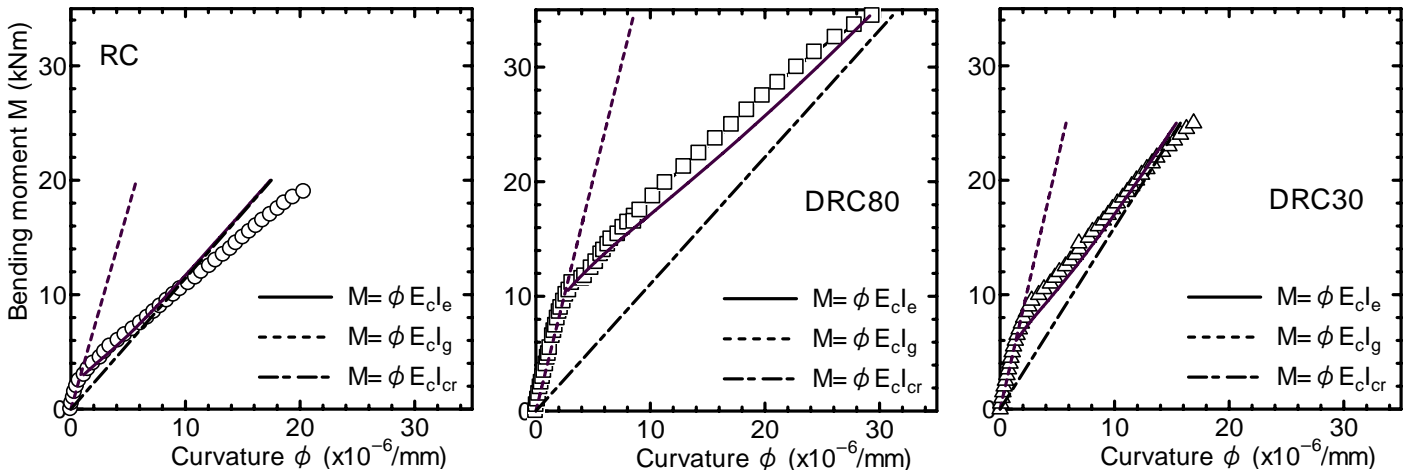


Figure 11. Comparison measured and calculated moment-curvature relationship of RC, DRC80 and DRC30

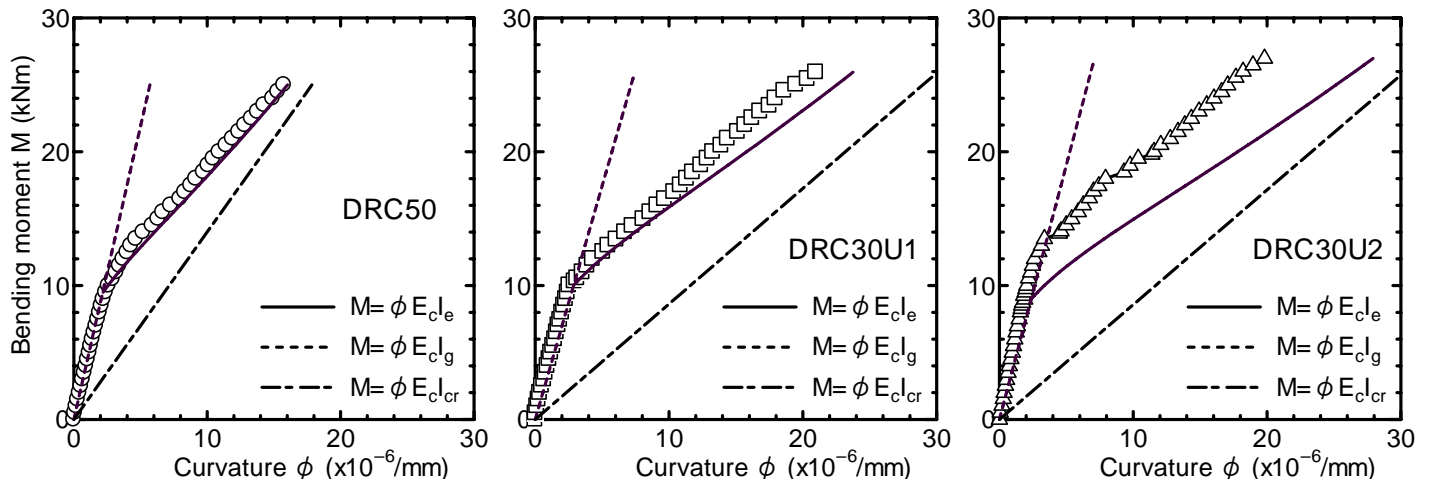


Figure 12. Comparison measured and calculated moment-curvature relationship of DRC50, DRC30U1 and DRC30U2

where, M_{max} is the moment in computation of curvature and is larger than M_{cr} . The measured values shown in Table 4 are used for the cracking moment M_{cr} in this study.

About RC, the calculated value using the effective moment of inertia well corresponds to measured value to the moment of about 10 kNm, however, from this point, the calculation becomes smaller than the measurement. On the other hand, the calculated values for the beams fortified with RPC are also in fair agreement with measured values until around the destruction except for DRC30U2. Fig.11 and Fig.12 indicate that RPC has little effect on the increase in curvature with the increase of bending moment after the generation of cracking. As already mentioned in the explanation on the behavior of reinforcement strain in the beam fortified with RPC, from the generation of cracking to the destruction of the beam, the width of crack developed in RPC is narrow. The constant stress corresponding to the first crack strength will be generated in RPC. Therefore, the internal force produced in RPC which resists the external moment may not change.

About DRC30U2, it is confirmed from the value of strain gauges affixed at the bottom surface of the beam that DRC30U2 beam cracked at the bending moment of 8.89 kNm. But, the crack does not affect the increase of curvature. In this connection, if 13.5 kNm of bending moment is used for cracking moment M_{cr} in Eq.(5), the calculation is in agreement with the measurement.

3.5 Capacity of beam

Table 5 shows the measured flexural capacity of specimen. The failure type of all beams was the tension failure that the yield of reinforcing bar precedes the failure of concrete, because the reinforcing bars in all specimens were designed as the under-reinforcement, In addition, although the

Table 5. Flexural capacity of specimens

Specimen	Flexural capacity (kNm)			$\sigma_{c,as}$ (N/mm^2)
	Measure- ment	Calcula- tion I	Calcula- tion II	
DRC80	34.5	37.81	34.16	3.04
DRC50	27.5	36.01	31.22	4.63
DRC30	25.5	31.72	27.04	7.12
DRC30U1	26.0	27.80	----	----
DRC30U2	28.5	27.12	----	----
RC	20.5	19.15		

$\sigma_{c,as}$: stress due to restraint of reinforcing bar against autogenous shrinkage of RPC

diagonal cracks which developed from the flexural cracks occurred in shear span of all specimens, that crack didn't influence the failure of the beam because of the arrangement of stirrups except for DRC30U2. Generally, diagonal cracking is the crack that flexural cracking is sloped by bending moment and shear force. The cracking moment of DRC30U2 is high and the cracking doesn't develop easily by the steel fiber in RPC. Therefore, the load on the initiation of diagonal cracks of DRC30U2 becomes high and DRC30U2 may have high shear capacity although stirrups aren't arranged at shear span in the beam.

The flexural capacity of the beams reinforced with RPC is larger than that of RC beam and increases with the increase of the area reinforced with RPC. This increase of flexural capacity may be due to RPC, however, the increasing ratio of flexural capacity isn't necessarily in proportion to the reinforced area of RPC. The calculation I is made according to the assumption on the distribution of stress shown at the right side of Fig.10. The calculated values for DRC30U1 and DRC30U2 are well in agreement with the measured values. However, the calculated values for DRC80, DRC50 and DRC30 are overestimated the measured values. In order to solve this overestimation, like the case of

the evaluation for the cracking moment of the beam fortified with RPC, the stress due to the restraint of the reinforcing bar against the autogenous shrinkage of RPC is also taken into consideration when calculating the flexural capacity of the beam reinforced with RPC. In the calculation II, the restraint stress generated in RPC is subtracted from the first crack strength of RPC. The calculated value of the flexural capacity of the beam reinforced with RPC is improved by the consideration of the restraint stress of RPC as shown in Table 5.

4 CONCLUSIONS

The reinforced concrete beam without cracking under serviceability limit state has been developed by authors. Flexural load tests of the beam fortified with RPC were carried out and the mechanical behaviors of the beams were investigated. The following conclusions are drawn within the scope of this study.

- 1) The cracks don't occur in the reinforced concrete beam fortified the tension zone with RPC suitably, when the moment corresponding to the generation of cracks below permissible crack width for corrosion of steel bar acts.
- 2) The cracking moment of the beam fortified with RPC can be evaluated by using the elastic analysis, provided that it is necessary to take the restraint stress into consideration when autogenous shrinkage of RPC is restrained.
- 3) The crack generated in the beam fortified with RPC is distributed by the steel fiber in RPC and the width of the crack is as small as 0.1mm or less from the generation of cracking to the destruction of the beam.
- 4) It is necessary to take into consideration that RPC shares the stress equivalent to first cracking strength of RPC for the evaluation of strain of reinforcing bar in the beam fortified with RPC after cracking.
- 5) The curvature of the beam fortified with RPC can be evaluated by the calculation using the effective moment of inertia like the case of the reinforced concrete beam.
- 6) The flexural capacity of the beam fortified with RPC is larger than that of the reinforced concrete beam and increases with the increase of the area reinforced with RPC.

REFERENCES

- JCI 2002 *Research committee report on performance evaluation and structural utilization of ductile fiber reinforced cementitious composites*. Tokyo: Japan Concrete Institute.
- JSCE 2002. *Standard specification for design and construction of concrete structures (Structural performance verification edition)*. Tokyo: Japan Society of Civil Engineers.
- JSCE 2004. *Recommendations for Design and Construction of Ultra High Strength Fiber Reinforced Concrete Structures*. Concrete Library 113. Tokyo: Japan Society of Civil Engineers.
- Katagiri, M., Maehori, S., Ono, T., Shimoyama, Y. and Tanaka, Y. 2002. Physical properties and durability of reactive powder composite material (Ductal). *Proceedings of the first fib congress 2002 Osaka*, pp.133-138.
- Musha, H. et al. 2002. Design and construction of SAKATA-MIRAI bridge using of reactive powder composite. *Bridge and Foundation Engineering* 36(11): pp.5-15
- Ujike, I et al. 2005. A study on crack prevention at service state of reinforced concrete member fortified tension zone by Reactive Powder Composite. *Journal of Society of Material Science* 54(8): pp.855-860